

# Chapter 5

## The Witten-Veneziano formula

---

In this chapter we attempt to compute  $F_\pi$  by means of a different method and we compare the result with the value obtained in the last chapter. The method relies on the Witten-Veneziano formula [1,2], which in 3-flavor QCD relates the mass of the  $\eta'$  meson with  $m_\eta$ ,  $m_\pi$ ,  $F_\pi$  and the *topological susceptibility*  $\chi_T$ , defined below. This formula is obtained from the leading order term of a  $1/N_c$  expansion, for large  $N_c$  (number of colors). The valence quark composition of  $\eta$  and  $\eta'$  is approximately

$$\eta \approx \frac{1}{\sqrt{6}} (\bar{u}u + \bar{d}d - 2\bar{s}s), \quad \eta' \approx \frac{1}{\sqrt{3}} (\bar{u}u + \bar{d}d + \bar{s}s). \quad (5.1)$$

In nature the  $\eta$  and  $\eta'$  states are mixed, so the actual composition is given in terms of a *mixing angle*  $\theta_P$

$$\begin{pmatrix} \eta \\ \eta' \end{pmatrix} = \begin{pmatrix} \cos \theta_P & -\sin \theta_P \\ \sin \theta_P & \cos \theta_P \end{pmatrix} \begin{pmatrix} \eta_8 \\ \eta_1 \end{pmatrix}, \quad (5.2)$$

where

$$\eta_8 = \frac{1}{\sqrt{6}} (\bar{u}u + \bar{d}d - 2\bar{s}s), \quad \eta_1 = \frac{1}{\sqrt{3}} (\bar{u}u + \bar{d}d + \bar{s}s). \quad (5.3)$$

$\eta_8$  belongs to an octet of states, while  $\eta_1$  to a singlet. The measured value of  $\theta_P$  is  $-11.3^\circ$  [3].

The Witten-Veneziano formula in QCD reads

$$m_{\eta'}^2 - \frac{1}{2}m_\eta^2 - \frac{1}{2}m_\pi^2 = \frac{6}{F_{\eta'}^2} \chi_T^{\text{que}}. \quad (5.4)$$

where  $F_{\eta'}$  is the decay constant of the meson  $\eta'$  and “que” stands for quenched, *i.e.* its value when the fermion mass  $m \rightarrow \infty$ . According to ref. [1], to lowest order in a  $1/N_c$  expansion, we have  $F_{\eta'} = F_\pi$  in QCD. In the limit of massless fermions, eq. (5.4) is simplified for the Schwinger model<sup>1</sup> [4,5]

$$m_\eta^2 = \frac{2N}{F_\eta^2} \chi_T^{\text{que}}, \quad (5.5)$$

where  $N$  is the number of flavors. Nevertheless, in this case the literature is not clear whether the approximation  $F_\eta = F_\pi$  is valid. Still, we assume that the relation between the decay constants holds and we attempt to compute  $F_\pi$  in the Schwinger model with eq. (5.5).

---

<sup>1</sup>According to the literature [4], the most suitable analogy of the heaviest meson of the Schwinger model with QCD would be  $\eta'$ ; however, it is not the actual  $\eta'$  particle from QCD and for simplicity we will denote it as  $\eta$ .

$\chi_T$  is defined for the Euclidean Schwinger model in the continuum as

$$\chi_T = \int d^2x \langle q(x)q(0) \rangle, \quad (5.6)$$

where

$$q(x) = \frac{g}{4\pi} \epsilon_{\mu\nu} F_{\mu\nu}(x) = \frac{g}{2\pi} F_{12}(x) \quad (5.7)$$

is the *topological charge density*. With  $q(x)$  we define the *topological charge* as

$$Q = \int d^2x q(x). \quad (5.8)$$

We can formulate  $\chi_T$  in terms of  $Q$  as well

$$\chi_T = \frac{\langle Q^2 \rangle - \langle Q \rangle^2}{V}, \quad (5.9)$$

where  $V$  is the space-time volume. An important property of the topological charge is that it is an integer number. We can see that fact if we rewrite  $q(x)$  as a total divergence

$$q(x) = \partial_\mu \Omega_\mu(x), \quad \Omega_\mu(x) = \frac{g}{2\pi} \epsilon_{\mu\nu} A_\nu(x). \quad (5.10)$$

If we consider field configurations of finite action,  $F_{\mu\nu}(x)$  has to vanish at infinity, so the gauge field must be gauge equivalent to 0 when  $|x| \rightarrow \infty$

$$0 = A'_\mu(x) = A_\mu(x) - \frac{1}{g} \partial_\mu \varphi(x). \quad (5.11)$$

Then

$$Q = \int d^2x \partial_\mu \left( \frac{g}{2\pi} \epsilon_{\mu\nu} \frac{1}{g} \partial_\nu \varphi(x) \right) = \frac{1}{2\pi} \int_{\partial\mathbb{R}^2} d\sigma_\mu \epsilon_{\mu\nu} \partial_\nu \varphi(x), \quad (5.12)$$

where we have used the Gauss theorem. Now, if we consider a circumference of length  $L$ , we identify  $Q$  with the following integral

$$\lim_{L \rightarrow \infty} \frac{1}{2\pi i} \int_0^L dx U^*(x) \partial_x U(x), \quad \text{where } U(x) = e^{i\varphi(x)}, \quad U(L) = U(0). \quad (5.13)$$

The last expression is equal to

$$\frac{1}{2\pi} [\varphi(L) - \varphi(0)] = n \in \mathbb{Z}, \quad (5.14)$$

hence  $Q$  is an integer.

As we mentioned in Chapter 3, we can relate  $m_\eta$  with the gauge coupling as follows

$$m_\eta^2 = N \frac{g^2}{\pi}. \quad (5.15)$$

Thus, by determining  $\chi_T$  we obtain a value for  $F_\pi$ . According to ref. [5], the theoretical expression for  $\chi_T^{\text{que}}$  in infinite volume and in the continuum is

$$\chi_T^{\text{que}} = \frac{g^2}{4\pi^2} \simeq 0.0253 g^2. \quad (5.16)$$

On the other hand, to measure the topological susceptibility by using lattice simulations we have to discretize the topological charge density. This can be done through the plaquette

Ref.	$\chi_T^{\text{que}}/g^2$	$F_\pi$
[5]	0.0253	0.3989
[8]	0.023	0.3801
[9]	0.0300(8)	0.4342(58)

Table 5.1: Topological susceptibility in the literature measured for  $\beta = 1/g^2 = 4$ . The results from refs. [8, 9] were obtained by means of lattice simulations, while in ref. [5]  $\chi_T^{\text{que}}$  corresponds to eq. (5.16).

variables defined in Chapter 2. From eq. (2.96), we know that for a small lattice spacing  $a$ , the plaquettes have the following expression

$$U_{\mu\nu}(\vec{n}) = e^{iga^2 F_{\mu\nu}(\vec{n})}. \quad (5.17)$$

Then

$$F_{\mu\nu}(\vec{n}) = -\frac{i}{ga^2} \ln U_{\mu\nu}(\vec{n}). \quad (5.18)$$

That way, we have

$$q(\vec{n}) = -\frac{i}{2\pi a^2} \ln U_{12}(\vec{n}) \quad (5.19)$$

and

$$Q = \sum_{\vec{n} \in L} a^2 q(\vec{n}), \quad (5.20)$$

where  $L = \{\vec{n} = (n_1, n_2) | n_\mu = 0, 1, \dots, N_\mu - 1; \mu = 1, 2\}$  is the set of lattice sites.

The lattice configurations generated through Monte Carlo algorithms are sorted in different sectors, where each one is characterized by a topological charge. Furthermore, there is evidence (see e.g. refs. [6, 7]) that the distribution of these configurations corresponds approximately to a Gaussian function. Due to parity symmetry, we also have that

$$\langle Q \rangle = 0. \quad (5.21)$$

Then, one can calculate  $\chi_T$  on the lattice using the following weighted average

$$\chi_T = \frac{\sum_i Q_i^2 N_i}{V \sum_i N_i}, \quad (5.22)$$

where  $i$  denotes a sector with  $N_i$  configurations labeled by a topological charge  $Q_i$ .

In the last chapter we showed results of  $Q$  obtained with simulations for several lattice sizes, using low statistics ( $10^3$  measurements separated by 10 sweeps). We attempted to compute the topological susceptibility using those results. Unfortunately, even though the topological charge is compatible with  $\langle Q \rangle = 0$ ,  $\chi_T$  as a function of the fermion mass  $m$  does not have a clear behavior (see figure 5.1 for instance). This does not allow us to perform a fit and to extrapolate to the quenched value of  $\chi_T$ . For that reason, we incremented the number of measurements to  $10^4$ , separated by 100 sweeps, and simulated a  $10 \times 64$  lattice for  $\beta = 4$ . This improved the results. In figure 5.2 we show the distribution of the configurations and in figure 5.3 we show the topological susceptibility as a function of the degenerate fermion mass. We used two functions to extrapolate  $\chi_T$ , from an average we obtain

$$\chi_T^{\text{que}} = 0.029(1)g^2. \quad (5.23)$$

Now, we substitute eq. (5.15) in eq. (5.5) and solve for  $F_\pi$

$$F_\pi^2 = \chi_T^{\text{que}} \frac{2\pi}{g^2}. \quad (5.24)$$

Using the result in eq. (5.23) yields

$$F_\pi = 0.4243(76). \quad (5.25)$$

$\chi_T$  has been obtained in the Schwinger model before. In table 5.1 we show some values available in the literature together with  $F_\pi$  computed by means of eq. (5.24). We observe that the topological susceptibility value in the literature is in the range 0.023-0.030 for  $\beta = 4$ , so our result is consistent.

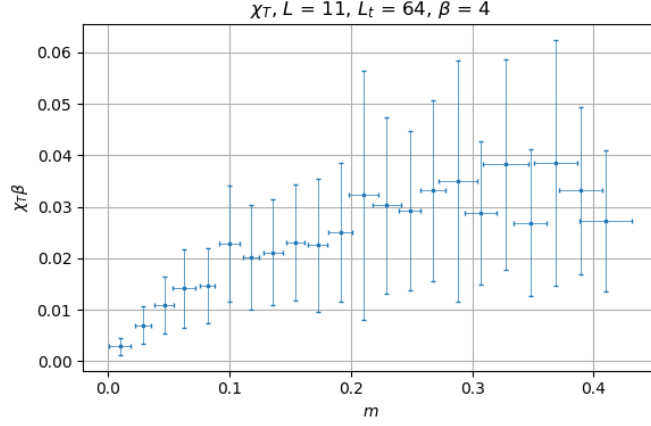
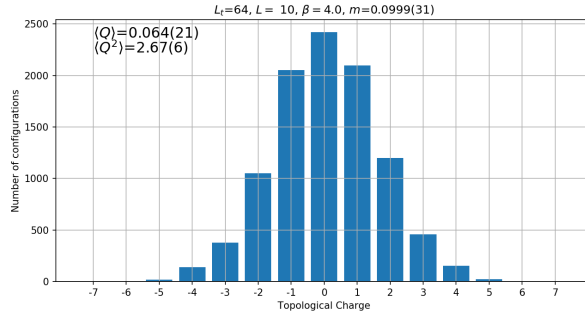
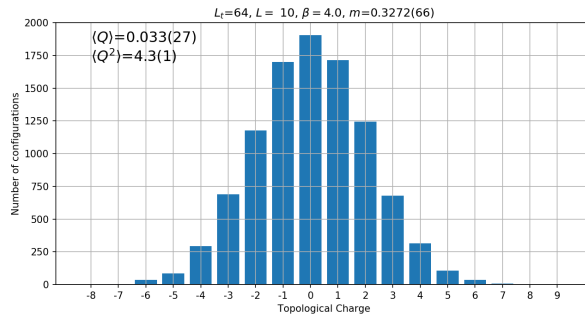


Figure 5.1: Topological susceptibility as a function of the fermion mass  $m$ , computed for  $10^3$  measurements with 10 sweeps between each of them on a  $11 \times 64$  lattice.  $\chi_T$  does not have a clear behavior for this amount of measurements.

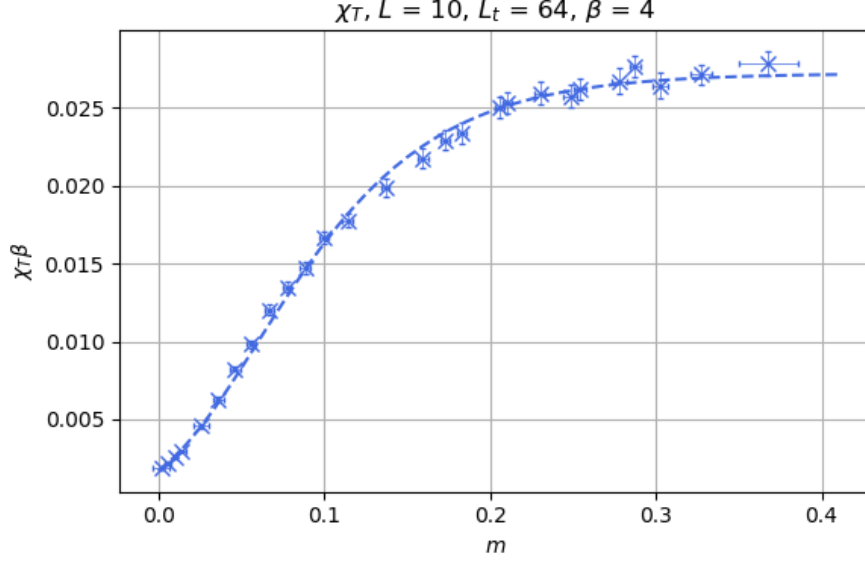


(a) Configurations sorted by their topological charge for  $m = 0.0999(31)$ .

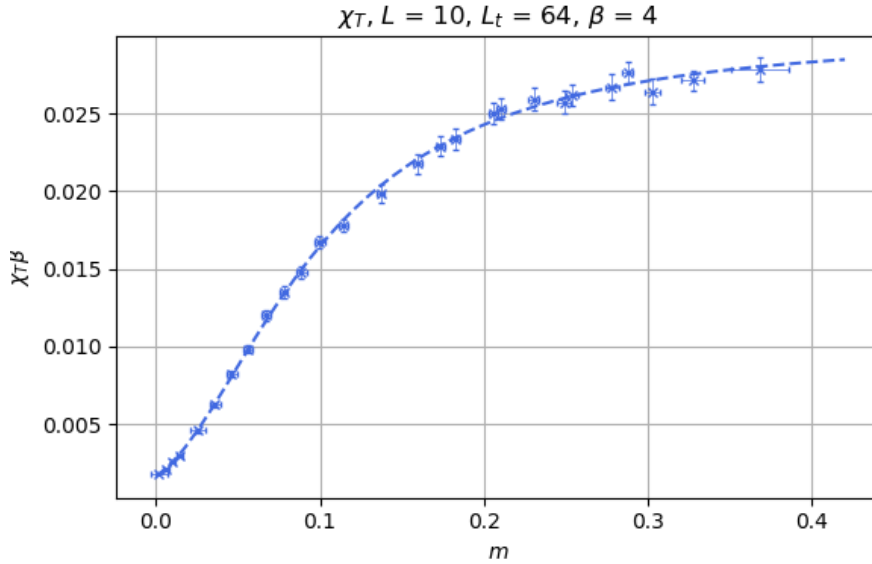


(b) Configurations sorted by their topological charge for  $m = 0.3272(66)$ .

Figure 5.2: Distribution of the Monte Carlo configurations in different topological sectors for  $\beta = 4$ . We see approximately a Gaussian distribution.  $m$  denotes the degenerate PCAC fermion mass. When the mass is smaller, the configurations occupy less topological sectors.



(a) A function of the form  $y = ae^{-be^{-cx}}$  was fitted to the data.



(b) We also fitted a function of the form  $y = \frac{a+bx+cx^2}{d+fx+gx^2}$ .

Figure 5.3: Topological susceptibility as a function of the degenerate fermion mass obtained with  $10^4$  measurements. The plots are in lattice unites. We performed two fits in order to extract the value of  $\chi_T$  when  $m \rightarrow \infty$ . The results yield  $\chi_T^{\text{que}}/g^2 = \chi_T^{\text{que}}\beta = 0.029(1)$ .

We also tried to verify that this result is independent of  $\beta$ . To do so, we performed more simulations to determine  $\chi_T$  in the quenched approximation by working with pure gauge theory, *i.e.* by generating Monte Carlo configurations using only the gauge action

$$S_G = \frac{1}{4} \int d^4x F_{\mu\nu} F_{\mu\nu}. \quad (5.26)$$

This is more convenient than extrapolating  $\chi_T$  to infinite  $m$ , because the simulations are faster and they yield results for  $m \rightarrow \infty$ . Still, the extrapolation of  $\chi_T$  to infinite  $m$  works as a cross-check with the results of  $\beta = 4$  that we obtain with the quenched simulations.

In figure 5.3, we show  $\chi_T^{\text{que}}\beta$  for different lattices of dimension  $L \times L$  and  $\beta = 2, 3, 4$  and 5. We took  $10^4$  measurements separated by 10 sweeps for  $\beta = 2, 3$  and  $10^4$  measurements separated by 100 sweeps for  $\beta = 4$  and 5. In table 5.2 we show  $\chi_T^{\text{que}}\beta$  for the different  $\beta$ 's that we simulated, together with  $F_\pi$  computed with the Witten-Veneziano formula.

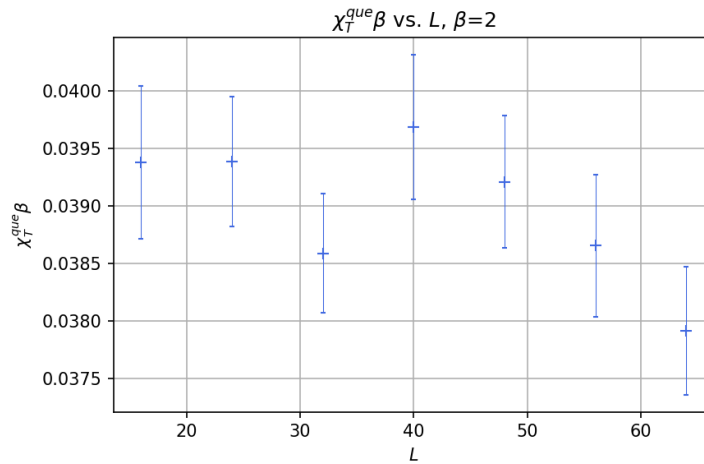
$\beta$	$\chi_T^{\text{que}}\beta$	$F_\pi$
2	0.0389(2)	0.495(1)
3	0.0335(3)	0.459(2)
4	0.0304(2)	0.437(1)
5	0.0285(4)	0.423(3)

Table 5.2: Results of  $\chi_T^{\text{que}}\beta$  and  $F_\pi$  for different  $\beta$ 's obtained with pure gauge theory simulations.

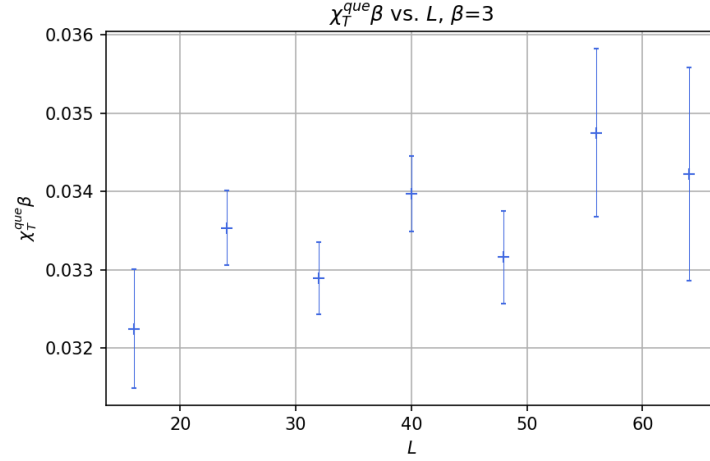
We expected  $\chi_T^{\text{que}}\beta$  on the lattice to be independent from  $\beta$ , as in the  $\delta$ -regime, but we observe that it is not the case. As  $\beta$  increases,  $\chi_T^{\text{que}}\beta$  decreases. For  $\beta = 4$  the number that we obtained by means of the quenched simulations is compatible, within errors, with the extrapolation that we performed before. In figure 5.4, we show a comparison of our results for  $\chi_T^{\text{que}}\beta$  with the values of refs. [5, 9]. We see that the lattice results are above the theoretical prediction, given by eq. (5.16), and they seem to converge to it for large  $\beta$ , which is the continuum limit. Since  $\chi_T^{\text{que}}\beta$  is not independent from  $\beta$ ,  $F_\pi$  is not independent either. Still, we can perform an extrapolation to the continuum limit by fitting the ansatz  $\chi_T^{\text{que}}\beta = a + b/\beta$ , where  $a$  and  $b$  are fit parameters, in order to determine  $F_\pi$ . The extrapolation yields

$$\frac{\chi_T^{\text{que}}}{g^2} = 0.0219(3), \quad F_\pi = 0.3707(23). \quad (5.27)$$

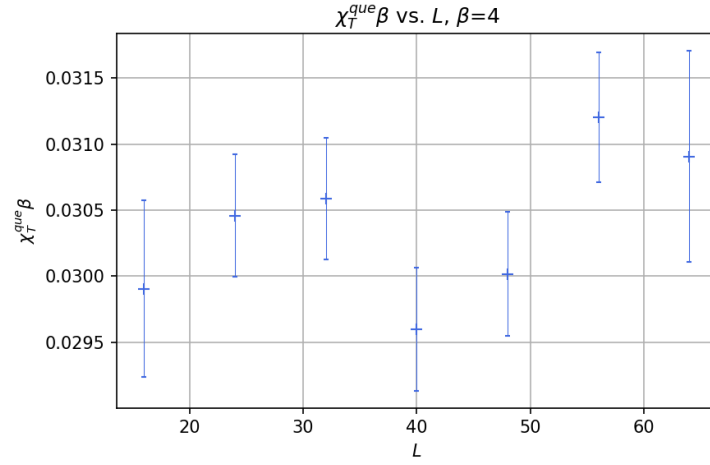
The result of eq. (5.27) is slightly below the theoretical prediction for infinite volume and in the continuum, given by eq. (5.16). Nevertheless, when we compare  $F_\pi$  with the value that we obtained in the  $\delta$ -regime:  $F_\pi = 0.6688(5)$ , we see an inconsistency between the two methods used to measure the decay constant. Furthermore, in the  $\delta$ -regime the result was independent of  $\beta$ , in contrast to the outcome of this chapter. However, let us remember that the actual decay constant involved in the Witten-Veneziano formula is the  $\eta$ . In the Schwinger model, the validity of the approximation  $F_\eta = F_\pi$  is not justified in the literature, so we cannot assure that we actually measured  $F_\pi$  in two dimensions with eq. (5.24).



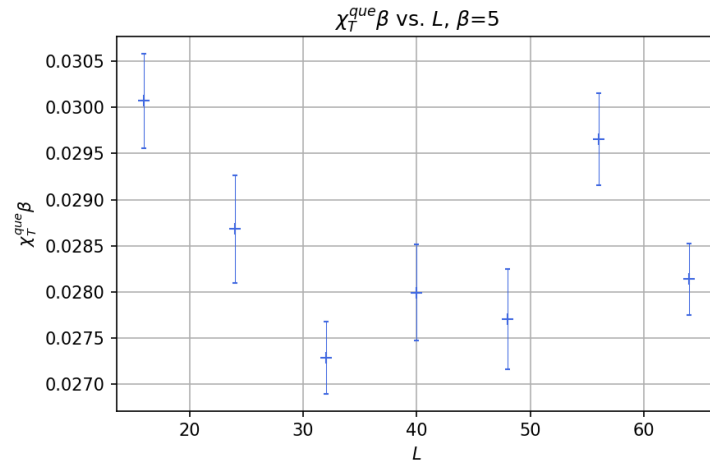
(a)  $\chi_T^{\text{que}}\beta$  vs.  $L$  for  $\beta = 2$ . An average yields  $\chi_T^{\text{que}} = 0.0389(2)$ .



(b)  $\chi_T^{\text{que}} \beta$  vs.  $L$  for  $\beta = 3$ . An average yields  $\chi_T^{\text{que}} = 0.0335(3)$ .



(c)  $\chi_T^{\text{que}} \beta$  vs.  $L$  for  $\beta = 4$ . An average yields  $\chi_T^{\text{que}} = 0.0304(2)$ .



(d)  $\chi_T^{\text{que}} \beta$  vs.  $L$  for  $\beta = 5$ . An average yields  $\chi_T^{\text{que}} = 0.0285(4)$ .

Figure 5.3:  $\chi_T \beta$  measured for different  $\beta$  and lattices of dimensions  $L \times L$

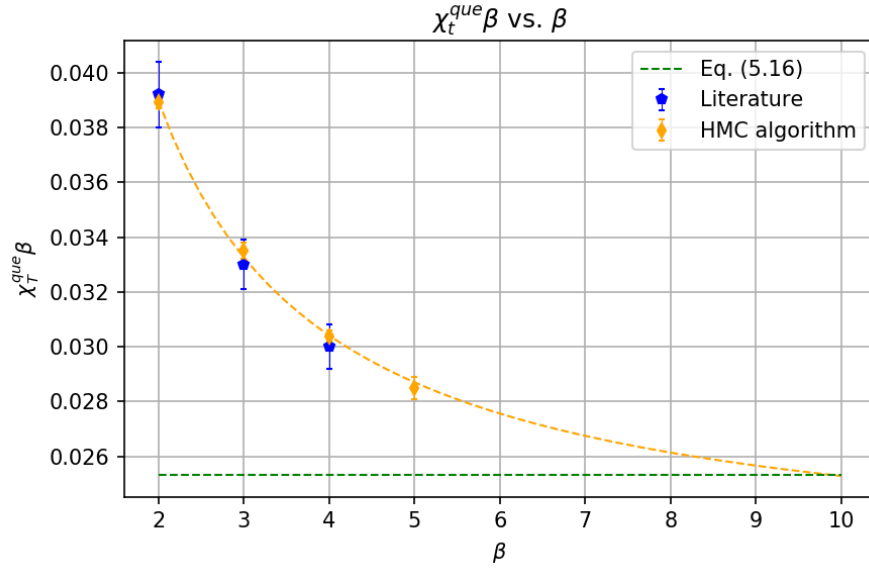


Figure 5.4:  $\chi_T^{que} \beta$  vs.  $\beta$ . The literature values correspond to ref. [9]. HMC algorithm denotes the results that we computed with pure gauge theory simulations. In order to determine  $\chi_T^{que} \beta$  in the continuum we fitted a function of the form  $y = a + b/x$ , which yielded  $\chi_T^{que} \beta = 0.0219(3)$ .



## *Bibliography*

---

- [1] E. Witten. Current Algebra Theorems for the U(1) Goldstone Boson. *Nucl. Phys. B*, 156:269–283, 1979.
- [2] G. Veneziano. U(1) Without Instantons. *Nucl. Phys. B*, 159:213–224, 1979.
- [3] P.A. Zyla et al. Review of Particle Physics. *Prog. Theor. Exp. Phys.*, 2020:083C01, 2020.
- [4] E. Seiler and I. O. Stamatescu. Some remarks on the Witten-Veneziano formula for the  $\eta'$  mass. *MPI-PAE-PTh-10-87*.
- [5] E. Seiler. Some more remarks on the Witten-Veneziano formula for the eta-prime mass. *Phys. Lett. B*, 525:355–359, 2002.
- [6] C. R. Gattringer, I. Hip, and C. B. Lang. Quantum fluctuations versus topology: A Study in U(1)-2 lattice gauge theory. *Phys. Lett. B*, 409:371–376, 1997.
- [7] S. Dürr, Z. Fodor, C. Hoelbling, and T. Kurth. Precision study of the SU(3) topological susceptibility in the continuum. *JHEP*, 04:055, 2007.
- [8] S. Dürr and C. Hoelbling. Scaling tests with dynamical overlap and rooted staggered fermions. *Phys. Rev. D*, 71:054501, 2005.
- [9] I. Bautista, W. Bietenholz, A. Dromard, U. Gerber, L. Gonglach, C. P. Hofmann, H. Mejía, and M. Wagner. Measuring the Topological Susceptibility in a Fixed Sector. *Phys. Rev. D*, 92:114510, 2015.